Isotopic composition of low-latitude paleoprecipitation during the Early Cretaceous

Marina B. Suarez[1†], Luis A. González[1], Gregory A. Ludvigson[2], Francisco J. Vega[3], Jesús Alvarado-Ortega[3]
[1]*Department of Geology, University of Kansas, 1475 Jayhawk Blvd., Lawrence, Kansas 66045, USA*
[2]*Kansas Geological Survey, University of Kansas, 1930 Constant Ave., Lawrence, Kansas 66047, USA*
[3]*Instituto de Geología, Universidad Nacional Autónoma de México, Ciudad Universitaria, Delegación Coyoacan, 04510, México City D.F., Mexico*

ABSTRACT

The response of the hydrologic cycle in global greenhouse conditions is important to our understanding of future climate change and to the calibration of global climate models. Past greenhouse conditions, such as those of the Cretaceous, can be used to provide empirical data with which to evaluate climate models. Recent empirical studies have utilized pedogenic carbonates to estimate the isotopic composition of meteoric waters and calculate precipitation rates for the Aptian-Albian. These studies were limited to data from mid- (35°N) to high (75°N) paleolatitudes, and thus future improvements in accuracy will require more estimates of meteoric water compositions from numerous localities around the globe. This study provides data for tropical latitudes (18.5°N paleolatitude) from the Tlayua Formation, Puebla, Mexico. In addition, the study confirms a shallow nearshore depositional environment for the Tlayua Formation. Petrographic observations of fenestral fabrics, gypsum crystal molds, stromatolitic structures, and pedogenic matrix birefringence fabric support the interpretation that the strata represent deposition in a tidal flat environment. Carbonate isotopic data from limestones of the Tlayua Formation provide evidence of early meteoric diagenesis in the form of meteoric calcite lines. These trends in δ^{18}O versus δ^{13}C were used to calculate the mean δ^{18}O value of meteoric water, which is estimated at −5.46 ± 0.56‰ (Vienna Standard Mean Ocean Water [VSMOW]). Positive linear covariant trends in oxygen and carbon isotopic values from some horizons were used to estimate evaporative losses of vadose groundwater from tropical exposure surfaces during the Albian, and the resulting values range from 8% to 12%. However, the presence of evaporative mineral molds indicates more extensive evaporation.

The added tropical data improve latitudinal coverage of paleoprecipitation δ^{18}O estimates. The data presented here imply that earlier isotope mass balance models most likely underestimated tropical to subtropical precipitation and evaporation fluxes. The limited latitudinal constraints for earlier isotope mass balance modeling of the Albian hydrologic cycle of the Northern Hemisphere Americas resulted in extrapolated low-latitude precipitation δ^{18}O values that were much heavier (up to 3‰) than the values observed in this study. The lighter values identified in this study indicate a more pronounced rainout effect for tropical regions and quite possibly a more vigorous evaporation effect. These and additional low-latitude data are required to better constrain changes in the hydrologic cycle during the Cretaceous greenhouse period, and to reduce the uncertainties resulting from limited geographic coverage of proxy data.

INTRODUCTION

The hydrologic cycle is a major variable in the evolution of the Earth system (Barron et al., 1989). Chahine (1992) suggested that most uncertainties in global-scale perturbations within the global climate system are due to inadequate understanding of the hydrologic cycle and its interactions with other parts of the global climate system. The persistence of these major scientific uncertainties about the extent to which precipitation and evaporation rates change in response to the forcing of higher global temperatures is highlighted by the recent findings of Zhang et al. (2007) and Graversen et al. (2008). Zhang et al. (2007) reported observations of recent increases in high-latitude precipitation rates and decreases in subtropical precipitation rates that are greater in magnitude than those estimated from general circulation models of global climate. Graversen et al. (2008) suggested that higher than expected Arctic temperature increases (i.e., "Arctic amplification") in both the lower and upper atmosphere might be the result of increased northward atmospheric transport of heat and moisture. If general circulation models originally tuned for modern climate forecasting do not capture the details of changes in the hydrologic cycle during the historic warming of the late twentieth century, then how can their performance be improved to better forecast the pending changes in precipitation and evaporation rates forced by near-range twenty-first century warming?

Paleoclimatologic studies that can better quantify the hydrologic cycles during past greenhouse conditions offer an empirical approach to better constrain the boundary conditions needed for fine-tuning climate models of near-range future climates. Meteoric δ^{18}O values calculated from isotopic compositions of pedogenic and freshwater carbonates have been used to better quantify the paleohydrologic cycle in the mid-Cretaceous greenhouse (Ludvigson et al., 1998; White et al., 2001; Ufnar et al., 2002, 2004; Poulsen et al., 2007). Ufnar et al. (2002) developed an oxygen isotope mass balance model based on meteoric δ^{18}O values of North American pedogenic sphaerosiderites (meteoric sphaerosiderite lines or MSLs). The model results indicate intensification of precipitation in the equatorial and mid- to high latitudes and intensification of evaporation in the subtropics. Ufnar et al. (2004) suggested that increased latent heat transport to the polar regions via an intensified hydrologic cycle contributed to Cretaceous polar warmth, as now proposed by Graversen et al. (2008) for modern arctic warming. The model, however, was based solely on pedogenic siderite

†E-mail: msuarez@ku.edu.

GSA Bulletin; November/December 2009; v. 121; no. 11/12; p. 1584–1595; doi: 10.1130/B26453.1; 8 figures; 3 tables;

data from the mid- (~35°N) to high latitudes (~75°N), and thus greater uncertainty is added by the lack of subtropical to equatorial empirical data with which to constrain the modeling exercise. To further test the accuracy and to improve on the findings of the mass balance modeling, it is imperative for the latitudinal empirical data to be expanded to tropical latitudes. The addition of low-latitude data is not only necessary to improve the mass balance–dependant precipitation and evaporation rates of the model used by Ufnar et al. (2002), but they are also needed to improve comparisons between proxy data and the general circulation models that now generate oxygen isotope estimates for precipitation (Poulsen et al., 2007).

Relevant data from the dry tropical to subtropical latitudes can be extracted from shallow-marine–supratidal carbonates that experienced early meteoric diagenesis. Micritic domains of exposed shallow-marine sediments frequently undergo early diagenetic stabilization by meteoric water in which the carbonate oxygen isotopic values are determined by the isotopic composition of mean annual rainfall, and the carbon values are modified by dissolved CO_2 derived from the oxidation of soil organic matter (Lohmann, 1988; Banner and Hanson, 1990). These diagenetic carbonates often produce unique systematic linear trends in $\delta^{13}C$ versus $\delta^{18}O$, defining meteoric calcite lines (MCLs sensu Lohmann, 1988), which are linear trends with more variable carbon isotopic values and invariant oxygen isotopic values.

The Albian Tlayua Formation in southern Mexico was considered an ideal candidate to capture tropical meteoric signals because it had been interpreted to represent a shallow-water back-reef lagoon with episodic freshwater input (Malpica-Cruz et al., 1989; Pantoja-Alor, 1992; Espinosa-Arrubarrena and Applegate, 1996; Applegate et al., 2006). However, at the onset of our investigation, Kashiyama et al. (2004) questioned the shallow freshwater-influenced interpretation and suggested an open-marine basin for the origin of the Tlayua Formation. Thus, a more rigorous petrographic evaluation and an expanded stable isotopic analysis was undertaken to determine the nature of Tlayua depositional environments. The results of our analyses confirm the shallow-marine to terrestrial depositional environment. Freshwater early diagenetic signatures allow us to extend the latitudinal meteoric $\delta^{18}O$ data into the tropics.

In addition to its contribution to global paleoclimate study, the Tlayua Formation at the Tlayua Quarry study site contains numerous well-preserved vertebrate and invertebrate fossils of mixed marine, freshwater, and terrestrial origin, as well as soft-tissue preservation (Martill, 1989; Pantoja-Alor, 1992; Applegate et al., 2006; Alvarado-Ortega et al., 2007). Isotopic and petrographic study provides further paleoenvironmental data to help understand this extraordinary paleontological resource.

GEOLOGIC SETTING

The Tlayua Formation, described by Pantoja-Alor (1992), crops out in the southern area of the Mexican state of Puebla known as Tepexi de Rodríguez (Fig. 1). In this area, late Paleozoic low-grade metamorphosed rocks (phyllites and schists) through early Tertiary sedimentary rocks rest on early Paleozoic tectonic fault blocks of the Acatlán Complex (Pantoja-Alor, 1992). This complex was an emergent area of land exposure during the Jurassic and possibly the Early Cretaceous (Applegate et al., 2006).

The Tlayua Formation consists of three carbonate members (Pantoja-Alor, 1992; Applegate et al., 2006). The Lower Member consists of at least 50 m of bluish-gray, massive micritic (mudstone to wackestone) limestone. This member is characterized by intraclasts, miliolids, 20–50-cm-high rudist biostromes, inoceramids, and chert concretions and lenses. The member is capped by a horizon of small bivalves and gastropods. The rudist *Toucasia polygyra* and the inoceramid *Chondrodonta* sp. were used to assign a lower Albian age to this member (Alencáster, 1973).

The Middle Member consists of 35 m of thinly bedded to laminated yellow-brown micritic limestone with reddish-yellow to purplish-red hematitic partings to thin hematitic clay layers. The Tlayua Quarry exposes most of the Middle Member, and it is from this unit that the majority of the well-preserved fossil material is found. The invertebrate fauna includes foraminifera, two unidentified sponges, two unidentified corals, bivalves, gastropods, cephalopods, arthropods (including arachnids, insects, isopods, decapod crabs, and ostracods), and echinoderms (see Applegate et al. [2006] for complete faunal and floral list). The fossil assemblage of the Tlayua Quarry is dominated (70%) by fishes of both marine and freshwater origin. Other vertebrate fossils include turtles, pterosaurs, crocodiles, and lizards (Reynoso, 1997, 2000, 2006). A few fragmentary plant fossils have also been recovered. Based on biostratigraphic and magnetostratigraphic analysis, the Middle Member is considered to be Albian (Benammi et al., 2006).

The conditions of preservation for the Tlayua Quarry have been, and continue to be, a subject of intensive study. The shallow, marginal marine hypothesis cites evidence for periodic exposure and freshwater influences and proposes the presence of stagnant, hypersaline environments and anaerobic conditions leading to superb preservation. Evidence includes algal mats, mud cracks, and the mixed marine, freshwater, and terrestrial fauna. The open-marine basin hypothesis of Kashiyama et al. (2004) suggests that deep water led to anaerobic to dysaerobic conditions that were responsible for preservation, and it suggests that stylolites and wavy pressure-solution features and/or the recrystallization of primary fabrics have mistakenly been identified as shallow-water indicators, such as algal mats.

The Upper Member of the Tlayua Formation is a truncated sequence of dolomite and dolomitic limestone. Petrographically, the Upper Member ranges from dolomite with intraclasts and miliolids to dolomite crystals in a micritic matrix (Pantoja-Alor, 1992). The miliolid species *Dicyclina schlumbergeri* was used to assign a Cenomanian age for this member (Pantoja-Alor, 1992). The Upper Member is truncated by overlying Cenozoic continental deposits.

METHODS

Samples were collected from the active quarry in the Middle Member at 1 m intervals (Fig. 2) and where there were distinct lithologic changes. In total, 27 samples were collected. Each sample was slabbed to produce two 1–3-cm-thick slabs. One of the two slabs for each sample was used to produce a 50 × 76 mm petrographic thin section, while the other slab was polished and used for isotopic sampling. Petrographic thin sections were used for identification of structures that could be used as indicators for a depositional environment, identification of diagenetic features, and identification of various carbonate domains for isotope sampling. Carbonates are classified using criteria of Folk (1962), with criteria from Dunham (1962) in parentheses. Stable isotope samples were milled from polished slabs using a microscope-mounted dental drill with 3–500-µm-diameter tungsten-carbide burrs to produce samples ranging from 25 to 100 µg, and samples were analyzed at the W.M. Keck Paleoenvironmental and Environmental Stable Isotope Laboratory at the University of Kansas. Individual beds were sampled repetitively to evaluate their unique intrinsic variability, and to define diagenetic trends in carbon-oxygen isotope space that yielded information about the paleohydrologic processes that led to stabilization of each bed. Samples were vacuum roasted at 200 °C for 1 h to remove volatile contaminants and analyzed using phosphoric acid digestion at 75 °C on a ThermoFinnigan Kiel III single-sample acid-dosing system connected to a ThermoFinnigan MAT 253 isotope-ratio mass spectrometer. Precision was monitored by daily

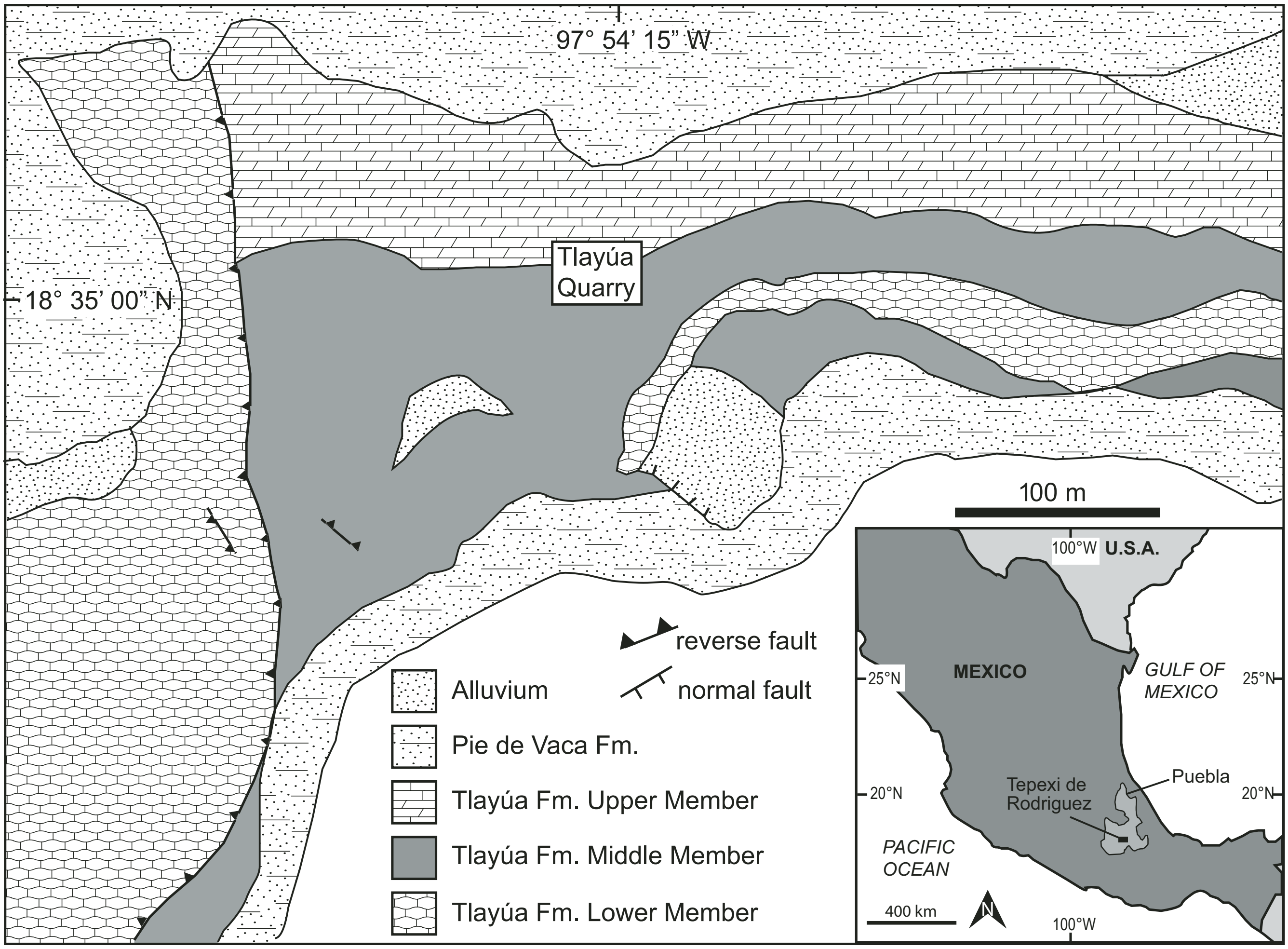

Figure 1. Local geologic map and location of the Tlayua Quarry in south-central Mexico (modified from Applegate et al., 2006).

analysis of NBS-18 and NBS-19 and was better than 0.1‰ for both carbon and oxygen. All carbonate data are reported relative to Vienna Peedee belemnite (VPDB), and isotopic compositions for water calculated from carbonate data are reported relative to Vienna Standard Mean Ocean Water (VSMOW). Confidence ellipses were generated using PAST (Paleontological Statistics software version 1.79; Hammer et al., 2008), and the principal axes of the ellipses were calculated using algorithms presented in Sokal and Rohlf (1995). All other statistics were calculated using the data analysis toolpack for Excel® 2008.

RESULTS

Petrography

Lower Laminated Facies

The lowermost 19 m of the section consist primarily of laminated to wavy laminated micrites (mudstones) and pelmicrites (wackestones) with hematitic (occasionally silty) partings. Many of the pelmicrites (wackestones) are characterized by fenestral fabrics (Fig. 3A), and some of the laminated to wavy laminated micrites (mudstones) are stromatolitic (Fig. 3B). Cyanobacteria filaments (Fig. 3C) are also present in the micrites and pelmicrites. Lenses to thin beds of foraminiferal biopelsparite (packstones) are less common than the pelmicrites and micrites, but they are consistently present in some of these units.

There are some notable exceptions to the laminated lithologies that dominate the lowermost 19 m. Samples 7 and 9 consist of a foraminiferal biopelsparite (packstone) that fines upward to a pelmicrite (wackestone). Sample 7 preserves a small part of a vertical *skolithos*-like burrow. A fossiliferous intrapelmicrite (wackestone) occurs at 16 m above the base of the section. This unit consists of a clotted texture of pelleted intraclast, abundant ostracodes and miliolid foraminifera, and a few micrite clasts (~1 cm) that contain common cyanobacterial filaments (Fig. 3D).

Upper Bedded Facies

The uppermost 7 m consist primarily of thin-bedded to thick-bedded micrite (mudstone) to pelmicrite (wackestone) and microspar, little to no hematitic partings are present, and foraminifera are less abundant. Micrite (mudstone) and dolomitized micrite characterized by distinct dolomite rhombs with calcitic centers (i.e., dedolomite) occur in samples 20, 21, and 25 (Fig. 4A). Sample 26 consists of massive micrite with abundant gastropods (wackestone). The uppermost part of the section (sample 27) has crinkly laminated fabric with micrite (mudstone), microspar, and sparry calcite (Fig. 4B). Secondary structures are common throughout the section, including soft-sediment deformation, microfaults, stylolites, silicified lenses, and calcite-filled veins.

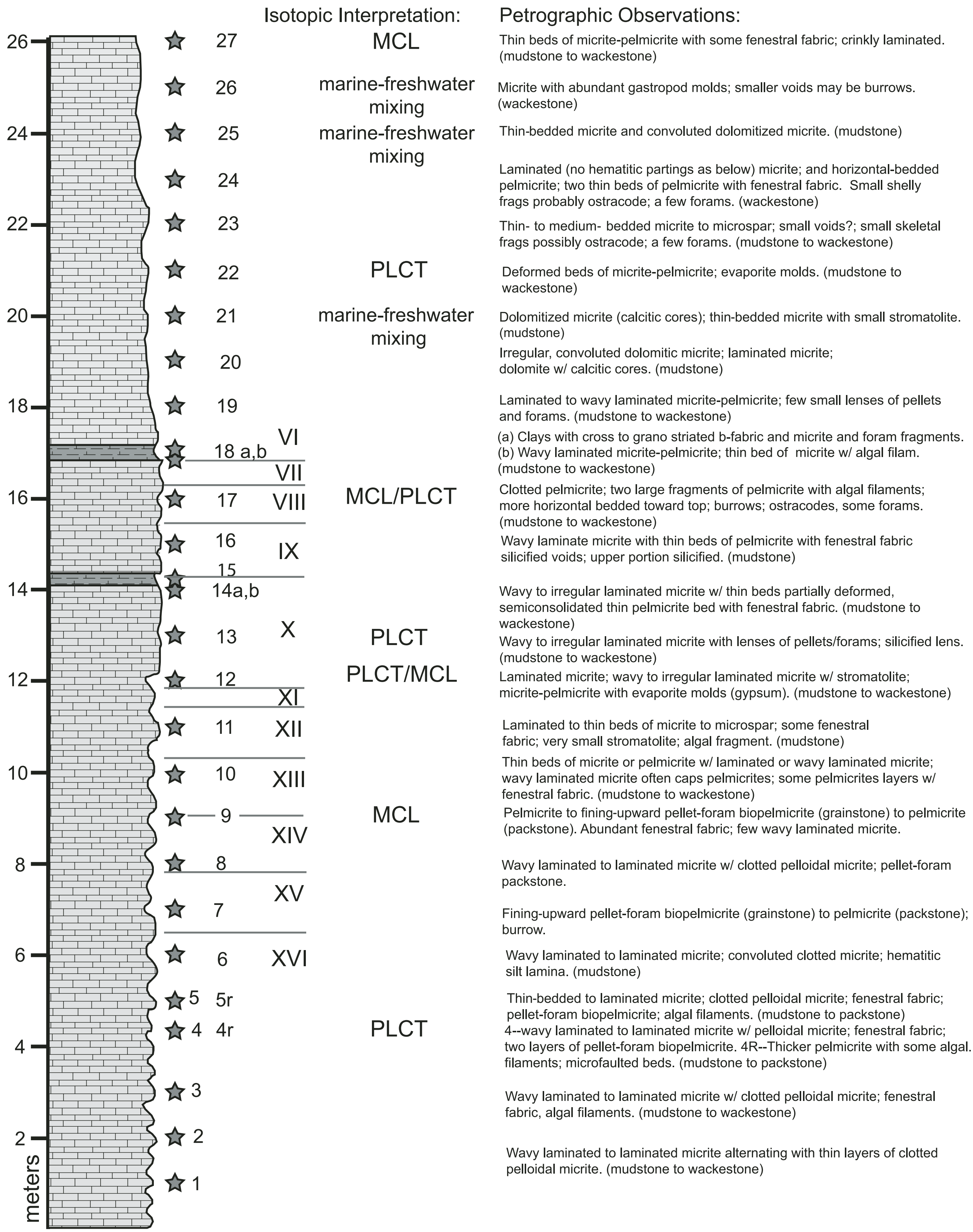

Figure 2. Lithologic profile of the Tlayua Quarry. Stars indicate sample positions. Roman numeral divisions are strata designations used by the quarry operators. The middle column indicates interpretation of carbonate isotopic composition indicative of either meteoric calcite lines (MCL) or positive linear covariant trends (PLCT). The right column contains petrographic observations.

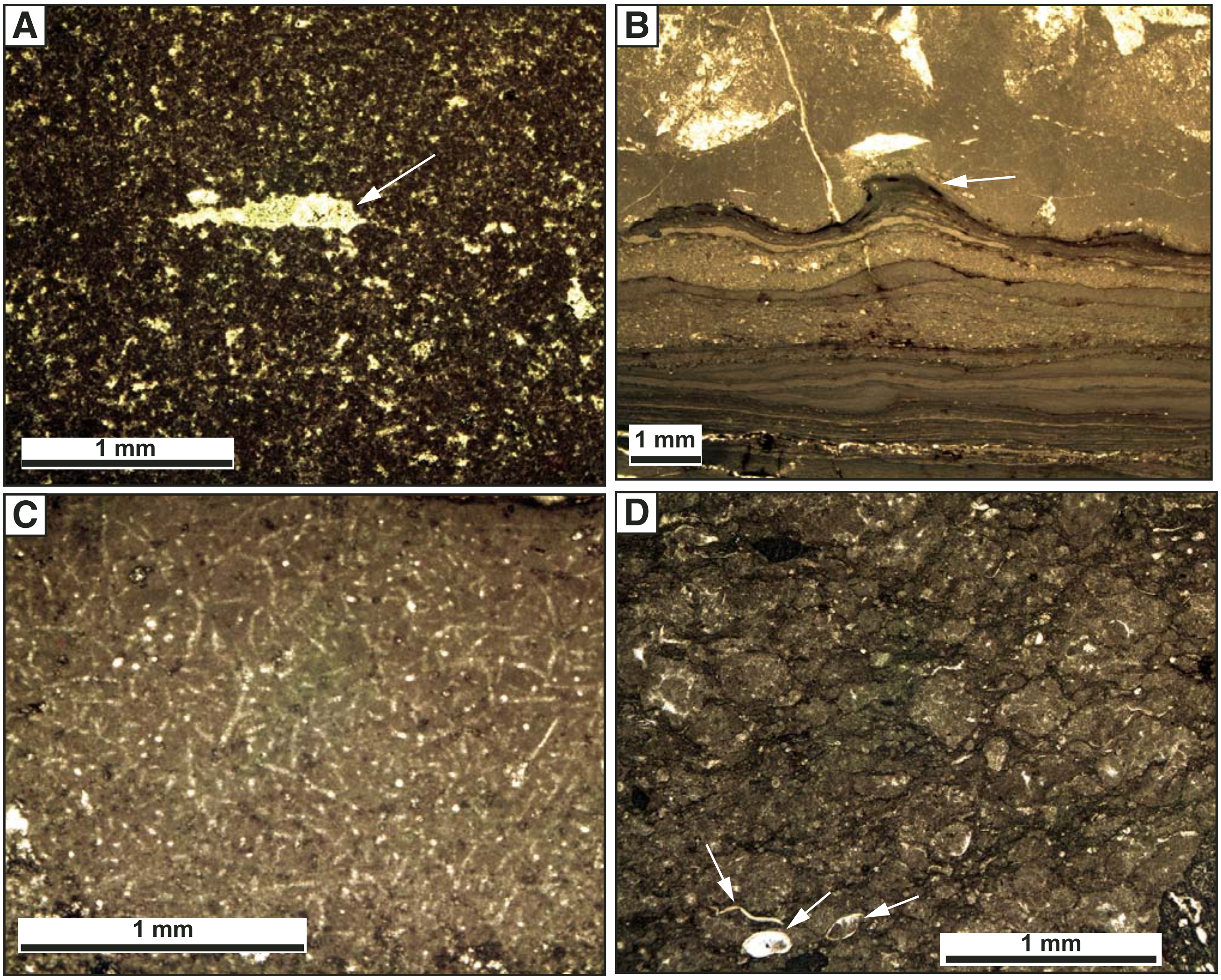

Figure 3. Features of the lower laminated facies. Photomicrographs were taken with plane polarized light. All scale bars are 1 mm. (A) Fenestral fabric (bird's eye structure) from sample 5 is indicated by arrow. (B) Laminated micrite and small stromatolite from sample 12 are indicated by arrow. (C) Cyanobacterial filaments from sample 5R. (D) Clotted micrite texture and ostracodes (indicated by arrow) in sample 17.

Evaporite Crystal Molds

Calcite-filled molds of gypsum crystals are found at 12 m (sample 12) and 21 m (sample 22) above the base of the section (Figs. 4C–4D). Sample 12 contains soft-sediment deformed laminations, while sample 22 consists of micro-faulted beds of micrite (mudstone) to pelmicrite (wackestone). These structures are important to note because they have not previously been documented in strata at the Tlayua Quarry.

Paleosols

Two calcareous clay layers are present in the Tlayua quarry. Both layers are 10–12 cm thick, and they occur at 14 and 17 m above the base of the section. A thin section of sample18a has a clay microstructure characterized by cross-striated birefringence fabric (b-fabric) to grano-striated b-fabric (Stoops, 2003) and abundant clasts of foraminiferal biomicrites (Figs. 4E–4F).

Isotopic Analysis

Over 300 carbonate microsamples were analyzed for carbon and oxygen isotopic composition. Most of these microsamples were extracted from micritic matrix to characterize the diagenetic trends in carbon-oxygen isotope space encoded by early diagenesis. To rule out possible overprinting effects by later diagenetic fluids, calcite veins and calcite spar-filled voids were also sampled.

The majority of the microsamples (302) were taken from micritic domains, and 22 microsamples were drilled from sparry calcite (13 from veins, 9 from voids). Overall, the isotopic data from micritic samples are widely scattered in $\delta^{13}C$-$\delta^{18}O$ crossplots, with an overall positive covariance (covariance = 1.94) (Fig. 5). The $\delta^{18}O$ values range from −11.67‰ to −0.39‰, and $\delta^{13}C$ values range from −8.45‰ to −0.89‰. Sparry domains in veins and void fills are also highly variable and generally more negative; $\delta^{18}O$ values range from −12.62‰ to −7.37‰, and $\delta^{13}C$ values range from −9.09‰ to −3.31‰. At least five MCLs were identified and are described later.

INTERPRETATION

Our petrographic and stable isotope analysis confirms the freshwater-influenced shallow-

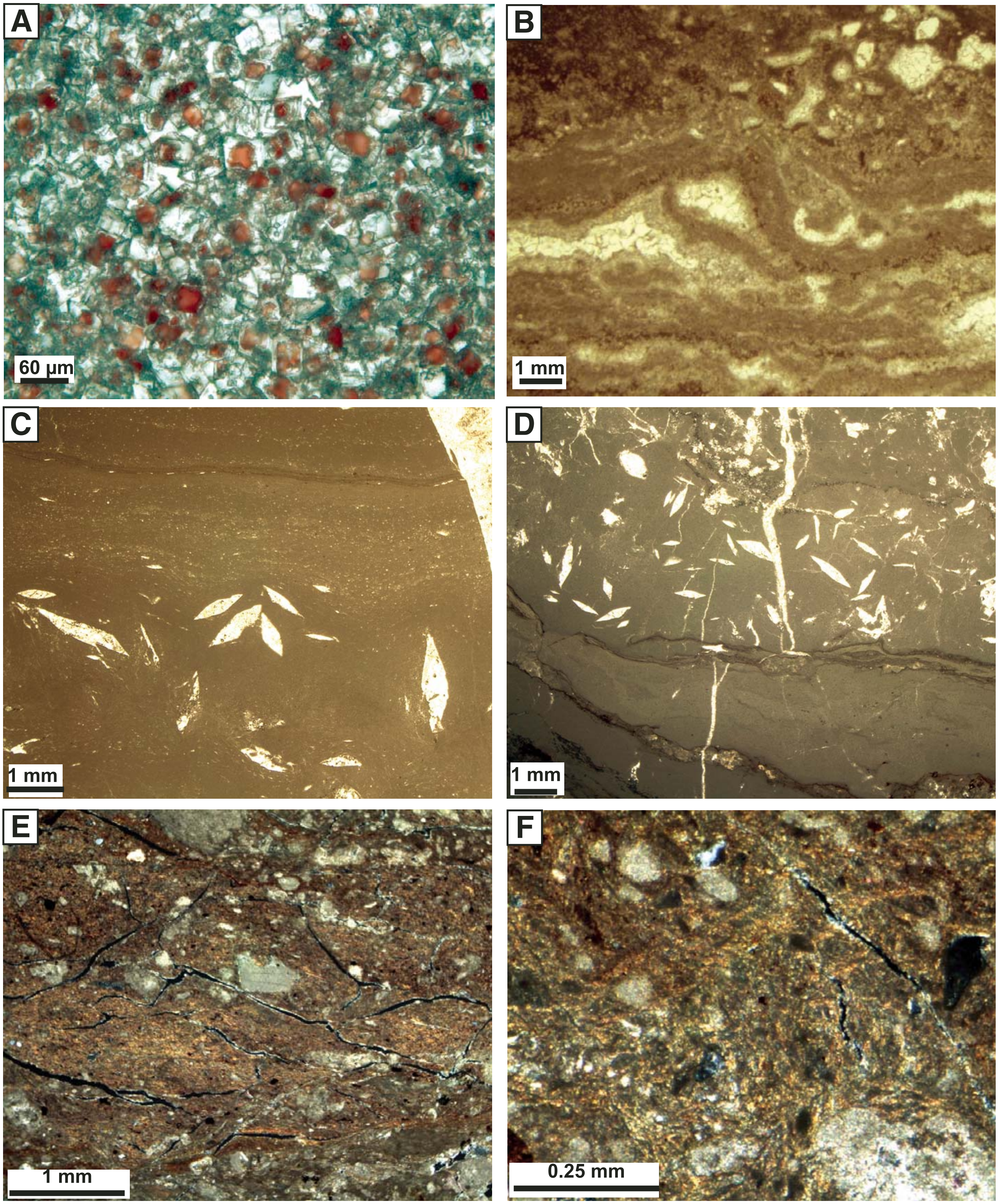

Figure 4. Features of the upper bedded facies, evaporites, and paleosols. Photomicrographs A to D were taken with plane polarized light. Photomicrographs E and F were taken with crossed-polarized light. (A) Dolomite with calcitic centers (stained red with Alizarin Red S) from sample 20. Scale bar is 60 µm. (B) Crinkly-laminated texture from sample 27. Scale bar is 1 mm. (C) Calcite spar-filled gypsum molds from lower laminated facies, sample 12. Scale bar is 1 mm. (D) Calcite spar-filled gypsum molds from the upper bedded facies, sample 22. Scale bar is 1 mm. (E) Micritic clasts surrounded by birefringence clays within the paleosol at sample 18A. Scale bar is 1 mm. (F) Photomicrograph showing cross-striated birefringent fabric and grano-striated birefringence fabric within the paleosol at sample 18A. Scale bar is 0.25 mm.

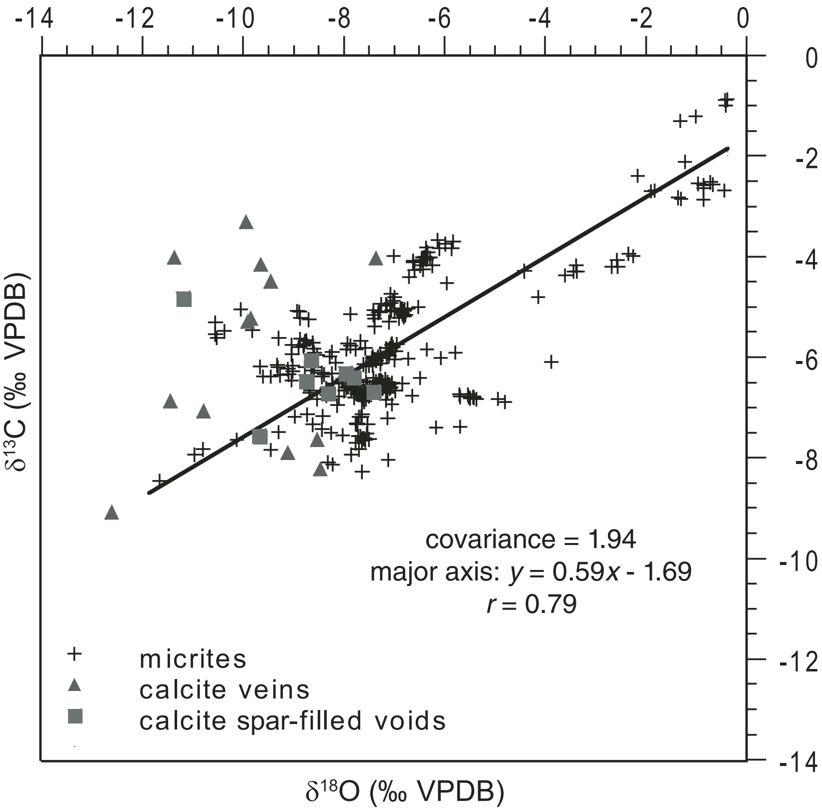

Figure 5. δ^{18}O versus δ^{13}C crossplot of all isotopic data from the Tlayua Quarry. Line indicates the major axis of a 95% confidence ellipse for all the micritic data. Overall, the micritic data are covariant (covariance = 1.94)

water coastal lagoon environments for strata in the Tlayua Quarry. The overall sequence represented at the Tlayua Quarry is specifically interpreted to range from subtidal lagoon deposits to the supratidal environments of a tidal flat (Fig. 6). Clay accumulations record pedogenesis and indicate sustained exposure of the strata to meteoric fluids leading to early diagenetic stabilization of micritic carbonate. This interpretation is based on a number of observations indicative of these environments.

Supratidal and Intertidal Environments

The majority of the structures observed in the Tlayua Quarry are indicative of supratidal to intertidal conditions. Many of the structures found in supratidal conditions can also form in the intertidal zone. Structures diagnostic of supratidal conditions (e.g., Shinn, 1983) that are present in thin section include cyanobacterial filaments, stromatolitic structures, fenestral fabrics, soil microstructure, and gypsum molds (Figs. 3 and 4).

A sustained period (i.e., tens to thousands of years) of emergence consistent with supratidal conditions is indicated by the presence of paleosols. Cross-striated to grano-striated b-fabrics in sample 18A (Figs. 4E–4F) suggest soil development (Retallack, 1997). The clay accumulation was likely the result of fluvial influx, and subsequent wetting and drying caused shrinking and swelling, resulting in the cross-striated b-fabrics (Brewer, 1964; Stoops, 2003).

Gypsum molds are also indicative of supratidal conditions and occur in samples 12 and 22. Gypsum suggests more arid sabkha-like conditions. It is also important to note that the gypsum molds retain their original euhedral crystal margins and are not collapsed, suggesting gypsum dissolution after early calcite cementation of the surrounding micritic matrix.

Evidence for a lower intertidal zone includes lenses and thin beds of marine benthic foraminifera (e.g., sample 4), ostracodes (e.g., sample 17), and bioturbation including vertical burrows (e.g., sample 7). Fining-upward biopelsparites (packstones to wackestones) layers are likely the result of storm deposition.

Subtidal Environments

Petrographic evidence for subtidal conditions includes massive micritic limestone (thoroughly bioturbated) (sample 26). The primary evidence for subtidal conditions is the variety of marine fauna found in the quarry described by previous authors. In addition to the marine fish found at the quarry, a diverse open-marine fauna have been described, including stenohaline organisms such as corals and echinoderms (Applegate et al., 2006), suggesting that in portions of the section, strata were deposited without major fluctuations in salinity (Heckel, 1972).

Isotope Geochemistry

Despite the wide spread in carbon and oxygen values of the micritic components, the isotopic evidence indicates that most of the strata in the Tlayua Quarry were diagenetically stabilized in tidal flat environments dominated by early meteoric (freshwater) diagenesis. Four of the hand samples (samples 9, 17, 18a, and 27) and two laminae in sample 12 display unique meteoric calcite lines (Fig. 7A). In addition to MCLs, linear trends with positive slopes, in which carbon and oxygen isotopic values trend along a covariant line, occur in samples 4r, 13, two lamina in sample 12, combined samples 17 and 18a, and sample 22 (Fig. 7B). Such trends have been described as "positive linear covariant trends" (PLCTs) (Sorensen et al., 2002; Davis et al., 2004; Ludvigson et al., 2004; Ufnar et al., 2008). These patterns are interpreted as evaporative trends, in which oxygen values were progressively enriched by preferential evaporation of ^{16}O-bearing water molecules. The carbon isotopes vary independently of the oxygen isotope and probably reflect kinetic effects from degassing of dissolved CO_2 originally derived from the oxidation of organic matter. When evaluated with coeval MCLs, the PLCTs can potentially indicate the extent of evaporative enrichment in the vadose zone during early diagenetic stabilization.

Meteoric Calcite Lines

The average δ^{18}O values of meteoric calcite lines for each sample that produced these trends are summarized in Table 1. A meteoric calcite line generated from the data from sample 9 is consistent with the petrographic evidence for fenestral fabric indicating early cementation in upper intertidal to supratidal conditions.

Within sample 12, four different laminae were microsampled, and four distinct populations of

TABLE 1. METEORIC CALCITE LINES

Sample	Average δ^{18}O (‰)	Standard deviation (‰)
9	–7.66	0.08
12a	–7.88	0.16
12d	–7.67	0.08
17/18A	–7.40	0.02
27	–8.71	0.17

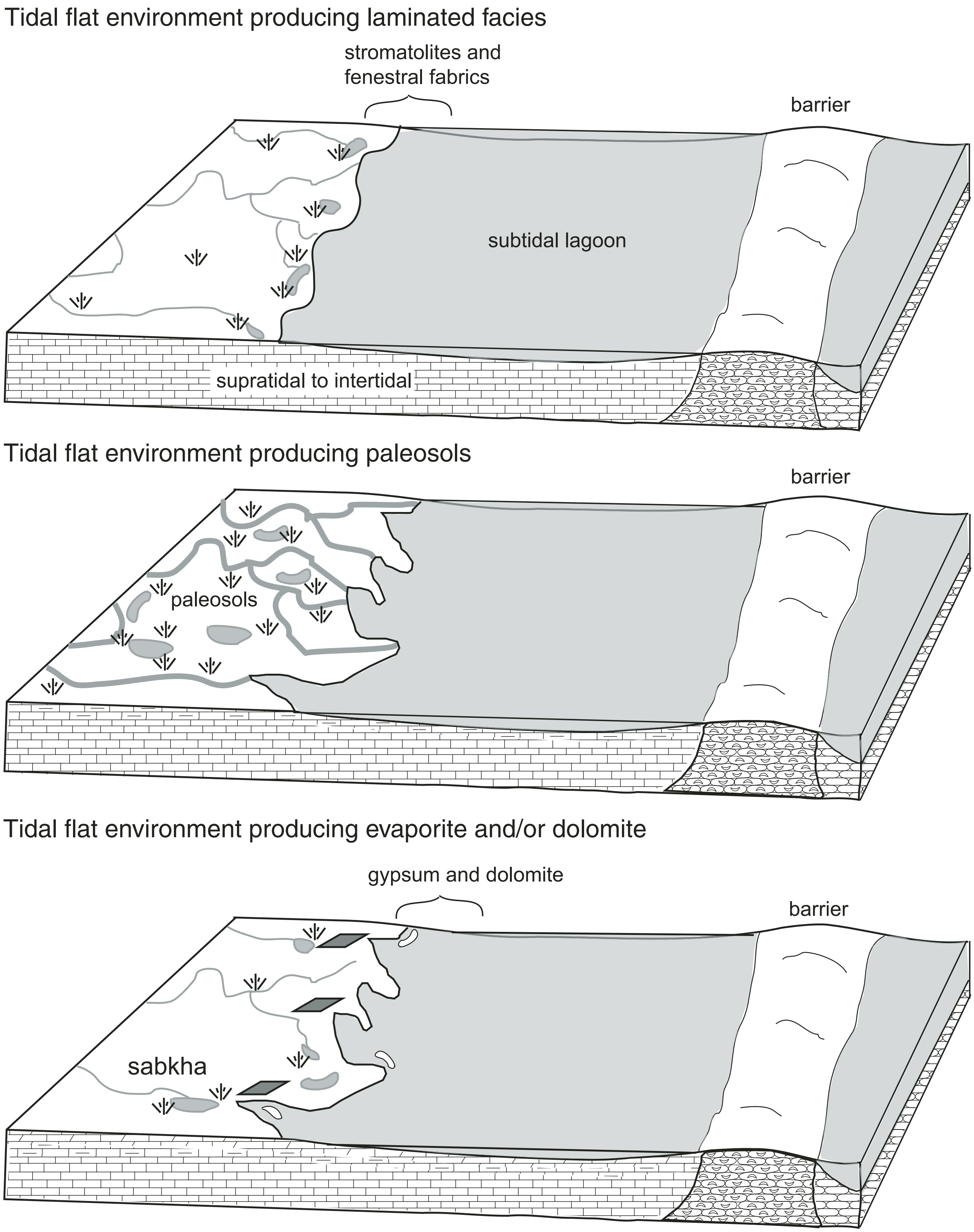

Figure 6. Schematic diagrams (not to scale) showing interpreted depositional environments for the Tlayua Quarry. Tidal flat environments existing behind a theoretical barrier as described in Applegate et al. (2006). Intertidal to supratidal conditions produced laminated facies. Paleosols developed on exposed surfaces in siliciclastic muds transported by fluvial discharge. Dolomite and evaporite facies likely occurred during more arid conditions in sabkha paleoenvironments.

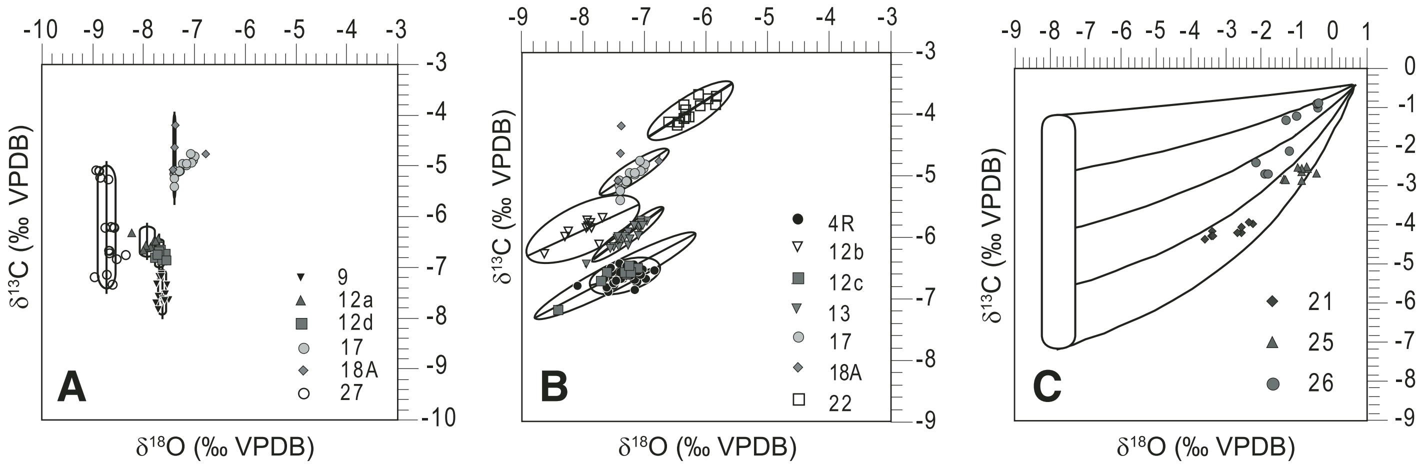

Figure 7. $\delta^{18}O$ versus $\delta^{13}C$ crossplots for diagenetic trends interpreted as meteoric calcite lines (MCLs), positive linear covariant trends (PLCTs), and marine-freshwater mixing. (A) Meteoric calcite lines. The averages of the MCLs are given by the vertical lines, with the standard deviation represented by the width of the rounded rectangles. (B) Data interpreted as PLCTs. The ellipses are the 95% confidence ellipses. Values for covariance and the coefficients and constants for the major axes of the 95% confidence ellipse are summarized in Table 2. (C) Data interpreted to have resulted from marine-freshwater mixing and modeled mixing curves. Data fall within hyperbolic arrays calculated using a marine fluid $\delta^{18}O$ of 3.50‰ (Vienna standard mean ocean water [VSMOW]) and a freshwater $\delta^{18}O$ of –5.46‰ (VSMOW) estimated from the average values of the MCLs. Curvature of the hyperbolic trends is determined by the amount and isotopic composition of dissolved inorganic carbon (DIC) in the respective paleogroundwaters. End-member seawater DIC is assumed to be 2.5 mmol/L with a $\delta^{13}C$ of –2.25‰ (Vienna Peedee belemnite [VPDB]). The DIC of freshwater end members ranges from 3.0 to 7.0 mmol/L, and $\delta^{13}C$ values range from –3.00‰ to –9.00‰ (VPDB). Temperature was held constant at 29 °C. The rounded rectangle represents the average MCL value (–7.78‰ ± 0.56‰ VPDB).

isotopic data were produced. The lowest (12a in Fig. 7A) and uppermost laminae (12d in Fig. 7A) sampled produced unique clusters of invariant $\delta^{18}O$ and $\delta^{13}C$ data. Two laminae between 12a and 12d (12b and 12c in Fig. 7B) display positive linear covariant trends. This rock sample clearly demonstrates the complexity and fine spatial scale of the deposition and early meteoric diagenesis that characterize these strata.

When plotted together, data from samples 17 and 18A (paleosol horizon) define a meteoric calcite line. In addition to the meteoric calcite line, a PLCT is also produced by the data from 17 and 18a (Fig. 7). We interpret that these patterns show that samples 17 and 18a were stabilized in the same phreatic-vadose paleogroundwater system.

Data from sample 27 also produce a meteoric calcite line, though it is somewhat more variable and is characterized by more negative $\delta^{18}O$ values (–8.71‰ ± 0.17‰). This sample is characterized by crinkly-laminated fabric associated with the presence of algal mats in supratidal conditions. These environments are ideal for early cementation by meteoric waters.

Positive Linear Covariant Trends

Data from samples that produce PLCTs are summarized in Table 2, which contains the covariance as well as the coefficients and constants for the line of the major axis of the 95% confidence ellipse. Like the samples that produce MCLs, the samples that produce PLCTs show petrographic features indicative of tidal flat depositional environments. These environments were influenced by infiltrating meteoric water and evaporative losses to the atmosphere. The isotopic compositions from a sample that define a MCL or a PLCT were probably governed by whether crystallization occurred in a shallow phreatic (MCL) or vadose (PLCT) paleogroundwater.

Marine Water–Freshwater Mixing

Isotopic data in samples 21, 25, and 26 have $\delta^{13}C$ and $\delta^{18}O$ values that are significantly heavier than those defining MCLs and PLCTs, and they are much closer to expected marine VPDB standard values. Their data can be modeled as covariant trends in carbon and oxygen isotope space that are arrayed along hyperbolic curves (Fig. 7C), which suggest mixing of marine and meteoric fluids (Lohmann, 1988). Specific hyperbolic trends result from differences in the concentrations of dissolved inorganic carbon in each end-member fluid (Lohmann, 1988). Samples 21 and 25 contain dolomitized micrite, which may also be consistent with mixing zone dolomitization (Shinn, 1983). Sample 26 is characterized by values that are closest to marine values. Oxygen isotopic values range from –2.17‰ to –0.39‰, and carbon isotopic values range from –2.69‰ to –1.00‰. These values were generated from a layer containing abundant gastropods, and they are probably indicative of restricted marine conditions. These more marine values were produced from strata in the upper bedded facies. These facies accumulated in environments that were more influenced by seawater than those of underlying units, and their depositional waters were also likely modified by evaporation. The depositional environment is still interpreted to have been tidal flats, but the freshwater influence that dominated lower in the section is muted in the upper portion, possibly due to more arid, sabkha-like conditions.

DISCUSSION

Implications for Depositional Environment

Identification of the depositional environments for the Tlayua Quarry strata has been the focus

TABLE 2. POSITIVE LINEAR COVARIANT TRENDS

Sample	Covariance	Slope	*Y* intercept	*R*
4R	0.01	0.27	–4.66	0.43
12b	0.03	0.49	–2.01	0.81
12c	0.08	0.52	–2.71	0.94
13	0.03	0.74	–0.57	0.93
17/18A	0.02	0.68	–0.18	0.88
22	0.03	0.62	–0.04	0.81

of many investigations since its discovery. It was important for this study to correctly identify the depositional environment in order to place the isotope data in an appropriate context for interpreting isotopic patterns, particularly since Kashiyama et al. (2004) raised doubts about the shallow marginal marine to coastal lagoon depositional environments postulated by previous authors. The majority of the isotopic and petrographic data presented here are consistent with the shallow marginal marine to coastal lagoon interpretation for the Tlayua Quarry deposits (Malpica-Cruz et al., 1989; Pantoja-Alor, 1992; Espinosa-Arrubarrena and Applegate, 1996; Applegate et al., 2006). Specifically, we identify the depositional environment as a tidal flat that included subtidal to supratidal subenvironments. Tidal flats occur in shallow marginal marine conditions, and coastal lagoons are common in tidal flat environments. We reject the open-marine hypothesis suggested by Kashiyama et al. (2004); however, the burial and/or tectonic diagenetic overprinting noted by Kashiyama et al. (2004) is recorded by some microfabrics and isotopic data. Kashiyama et al. (2004) suggested that these features were misinterpreted by others as evidence for shallow-marine deposition. Stylolites are indeed abundant in thin section, but under petrographic examination, they can be easily distinguished from the stromatolitic features. We found ample field, petrographic, and geochemical evidence of freshwater influence, exposure, and alteration by meteoric fluids. In addition, the calcite vein and calcite spar void fills were dominated by the lightest $\delta^{18}O$ values, and a number of micritic samples had similar light values with much greater ranges of $\delta^{18}O$ variability (samples 1–4, 5–8, 10, 11, 14–16, 19, 20, and 22–24), suggesting that some of the micritic values were influenced by later diagenetic fluids (Lohmann, 1988). Despite the late diagenetic overprinting on the isotopic composition of many of the micrites, well-defined MCLs and PLCTs are easy to distinguish in some of the horizons (Fig. 7). The abundant red clays were likely the result of transportation and discharge from fluvial runoff. A detailed spectral analysis of the microfacies at the Tlayua Quarry conducted by Kashiyama et al. (2004) showed evidence of Milankovitch cyclicity, which was interpreted to indicate a precessional cycle that was modified due to a double-monsoon effect. They argued that this effect was due to the geographic position of the Tlayua Quarry during the Early Cretaceous between the northern and southern American continents. Such monsoon effects would be a logical mechanism to explain delivery of the red clay sediments into the Tlayua shallow coastal lagoon. Moreover, pedogenesis in the red clays clearly indicates that these are nearshore deposits that were modified by terrestrial environments during minor sea-level fluctuations.

Estimates of Groundwater $\delta^{18}O$ Values

The early meteoric diagenetic signals identified in the Tlayua Quarry deposits allow us to estimate the composition of meteoric water, which is equivalent to local precipitation (Lohmann, 1988) during the deposition of the Middle Member of the Tlayua Formation. We utilized the second-order polynomial regression generated by Ufnar et al. (2002) from the latitudinal temperature gradient presented by Spicer and Corfield (1992) and based on fossil leaf physiognomy data of Wolfe and Upchurch (1987):

$$t = 30.25 - 0.2025l - 0.0006l^2,$$

where t is temperature in degrees Celsius, and l is latitude. There are no independent paleotemperature data from the Tlayua Quarry site. Thus, we utilized the terrestrial temperature gradient based of fossil leaf data rather than other temperature gradients because plants are directly in contact with atmospheric conditions and because this data set provides purely empirical data that are independent of modeled latitudinal temperature gradients. As shown by Spicer and Corfield (1992), the empirical Cretaceous terrestrial and sea-surface temperature gradients are not significantly different. In addition, the temperature estimate compares well to modeled mean annual temperatures from 18°N to 19°N at two times modern pCO_2 levels (Poulsen et al., 2007).

The Tlayua Quarry site is estimated to have been located between 18°N and 19°N during the Cretaceous, based on paleogeographic reconstructions (e.g., Meschede and Frisch, 1998) and paleomagnetic data (Benammi et al., 2006). At these latitudes, the leaf physiognomy–based mean annual temperature estimate is ~26 °C. The calcite-water ^{18}O fractionation factor (α) calculated from the relationship reported by Friedman and O'Neil (1977) was used with the estimated temperature to determine the $\delta^{18}O$ values of the meteoric fluids at Tlayua Quarry. The isotopic compositions of the meteoric waters that produced the MCLs in sample 9, the two laminae in sample 12, combined samples 17 and 18a, and sample 27 are estimated at –5.34‰, –5.57‰, –5.36‰, –5.09‰, and –6.40‰ (Vienna standard mean ocean water [VSMOW]), respectively.

The data generated in this study produce Cretaceous tropical groundwater $\delta^{18}O$ values that improve latitudinal groundwater $\delta^{18}O$ trends (Fig. 8) estimated from Cretaceous pedogenic siderite (Ufnar et al., 2002; Suarez et al., 2007) and pedogenic calcite (Ludvigson et al., 2004; Ufnar et al., 2005). These new tropical-subtropical data (this study; Suarez et al., 2007) indicate lighter $\delta^{18}O$ compositions than values produced by projecting the initial mid-latitude to polar trend generated by Ufnar et al. (2002), which produced a meteoric water composition ~3‰ heavier (–2.08‰ VSMOW) than the values estimated from the Tlayua Quarry carbonates. This suggests that greater rainout effects would be needed to produce the more depleted values observed in this study. Our estimates of $\delta^{18}O$, ranging from –5.09‰ to –6.40‰, however, are similar to the ~–4.0‰ to –7.0‰ modeled by Poulsen et al. (2007) for this latitude.

Estimates of the Extent of Tropical Evaporation

The PLCTs allow us to estimate minimum amounts of evaporation needed to produce the more enriched carbonate $\delta^{18}O$ values from ancient tidal flats in the Tlayua Quarry section by using a simple Rayleigh distillation approach (Table 3). The $\delta^{18}O$ of meteoric groundwater for each PLCT was calculated using the most depleted calcite $\delta^{18}O$ value for each PLCT. The Rayleigh distillation approach was used to determine what fraction must be evaporated and lost to the atmosphere in order to produce the most enriched PLCT values:

$$\delta_l = (\delta_{lo} + 1000) f^{(\alpha_{l-v} - 1)} - 1000,$$

where δ_l is the final liquid isotopic composition (calculated from the most enriched PLCT value), δ_{lo} is the isotopic composition of the initial fluid (calculated from the most depleted PLCT value), f is the fraction remaining, and α is the fractionation factor of liquid from vapor (Gonfiantini, 1986). For all of the PLCT trends, 8%–12% of the groundwater must be evaporated to produce the most enriched values. It should be noted that these values reflect evaporation in the vadose zone during early meteoric diagenesis of the tidal flat sediments. It is likely that even greater evaporation effects occurred during the deposition of the tidal flat sediments that contain gypsum molds. Indeed the 8%–12% estimate of evaporation may be an underestimate, since Ufnar et al. (2008) recently demonstrated that the PLCT offset from the MCL, and thus the slope of the PLCT, is significantly controlled by the calcite saturation and pCO_2 of the precipitating fluid. For fluids that degass quickly, calcite precipitation can occur before the fluid undergoes significant evaporation, and before the fluid can become extremely enriched in ^{18}O, and thus calcite might not record the full extent of evaporative enrichment (i.e., the PLCT). In general, our findings are consistent with the modeling study

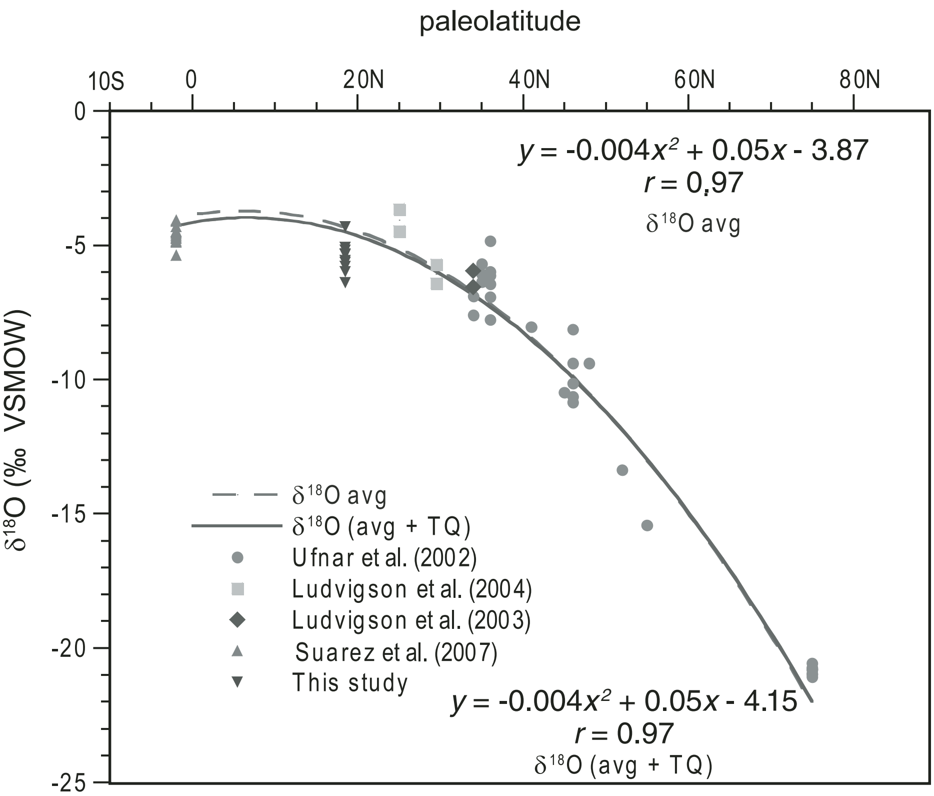

Figure 8. Latitudinal gradient for $\delta^{18}O$ of mid-Cretaceous meteoric water estimated from the isotopic composition of pedogenic or early diagenetic carbonates (siderite or calcite). Each symbol represents the oxygen isotopic composition of meteoric water calculated from the average value of a meteoric calcite line (MCL) or a meteoric sphaerosiderite line (MSL) at a given latitude. The dashed line is a second-order polynomial fit to the average estimated groundwater $\delta^{18}O$ value for each latitude based on Ufnar et al. (2002; MSL based), Ludvigson et al. (2003; MCL based), Ludvigson et al. (2004; MCL based), and Suarez et al. (2007; MSL based). The solid line is the second-order polynomial fit to all the data including the Tlayua Quarry data.

TABLE 3. CALCULATION OF PERCENT EVAPORATION VIA RAYLEIGH DISTILLATION

Sample	δ_{lo}	δ_{l}	α	f	% evaporation
4R	–5.79	–4.53	1.029	0.89	11%
12b	–6.31	–5.27	1.029	0.90	10%
12c	–6.11	–4.82	1.029	0.88	12%
13	–5.64	–4.64	1.029	0.91	9%
17/18A	–5.09	–4.45	1.029	0.94	6%
22	–4.31	–3.52	1.029	0.92	8%

on Cretaceous (Wealden) climates by Haywood et al. (2004) that argues for development of evaporation deficits despite large increases in zonal Cretaceous precipitation.

CONCLUSIONS

Petrographic and isotopic data from the Tlayua Formation at the Tlayua Quarry indicate that the quarry strata were deposited in a tidal flat–shallow lagoon system that was often subject to freshwater influx from precipitation and fresh groundwater discharge. Evidence for tidal flat–shallow lagoon systems includes fenestral fabrics, gypsum molds, cyanobacterial and stromatolitic structures, a fauna that includes a mixture of marine organisms with terrestrial and freshwater aquatic fauna, and isotopic signatures characteristic of early meteoric diagenesis. Paleosols and their matrix micromorphology are clear indicators of subaerial exposure at Tlayua, and the associated red clay accumulations indicate frequent influence of fluvial deposition during the monsoon months.

MCLs and PLCTs that are unique to meteoric environments yield an estimate average $\delta^{18}O_{(VSMOW)}$ value of early meteoric diagenetic fluids of –5.46‰ ± 0.56‰ and a minimum estimate for evaporative loss of groundwater at 8%–12%. These estimates for isotopic composition of precipitation are consistent with the geometry of modern latitudinal trends, which show a plateau in the subtropical regions. The trends generated by the limited mid- to high-latitude data used in the model of Ufnar et al. (2002) projected much heavier precipitation $\delta^{18}O$ values in the subtropical and tropical regions. The data presented here imply that the earlier model might have underestimated tropical to subtropical precipitation and evaporation fluxes due to the inaccurate precipitation $\delta^{18}O$ value extrapolated from the high-latitude data. The lighter values estimated in this paper would require greater rainout to cause the depletion of $\delta^{18}O$ of meteoric water and possibly much higher evaporation rates to sustain the aridity that prevailed in the region as suggested by the presence of evaporite minerals. Estimates of the impact on evaporation fluxes and latent heat transport calculations (Ufnar et al., 2004) require that model runs be carried out with the constraints afforded by the Tlayua data and the other low-latitude data being generated by our group (e.g., Suarez et al., 2007).

Our results suggest that oxygen isotopic compositions of pedogenic carbonates and early diagenetic carbonate cements provide reliable paleoclimatic data with which to calibrate empirical and numerical models used to simulate ancient and future climate. Moreover, it is imperative that we expand empirical data acquisition into the Southern Hemisphere, where Cretaceous data are currently nearly nonexistent, and modeled precipitation and evaporation values are not constrained.

ACKNOWLEDGMENTS

We wish to express appreciation to Luis Garibay for assistance in the field. In addition, sample preparation and isotopic analysis were assisted by Michael Bruemmer, Gregory Cane, Stacy Rosner, Ian Rowell, Celina Suarez, and Zachary Wenz. We thank Luis Espinosa-Arrubarrena and the late Shelton P. Applegate for sharing their knowledge of Tlayua Quarry fauna with us. Mouloud Benammi graciously shared with us samples used in his magnetostratigraphic study. This manuscript benefited from insightful reviews by Hope Jahren and Troy Rasbury. This study was supported by National Science Foundation grant EAR-0325072 to González and Ludvigson.

REFERENCES CITED

Alencáster, G., 1973, Una nueva especie de *Toucasia* en el Cretácico medio de los estados de Oaxaca y Puebla: Paleontología Mexicana, v. 36, p. 1–20.

Alvarado-Ortega, J., Espinosa-Arrubarrena, L., Blanco, A., Vega, F.J., Benami, M., and Briggs, D.E.G., 2007, Exceptional preservation of soft tissues in Cretaceous fishes from the Tlayua Quarry, central Mexico: Palaios, v. 22, p. 682–685.

Applegate, S.P., Espinosa-Arrubarrena, L., Alvarado-Ortega, J., and Benammi, M., 2006, Revision of recent investigations in the Tlayua Quarry, *in* Vega, F.J., Nyborg, T.G., Perrilliat, M.C., Montellano-Ballesteros, M., Cevallos-Ferriz, S.R.S., and Quiroz-Barroso, S.A., eds., Studies on Mexican Paleontology: Topics in Geobiology: Dordrecht, Springer, p. 275–304.

Banner, J.L., and Hanson, G.N., 1990, Calculation of simultaneous isotopic and trace-element variations during water-rock interaction with applications to carbonate diagenesis: Geochimica et Cosmochimica Acta, v. 54, p. 3123–3137, doi: 10.1016/0016-7037(90)90128-8.

Barron, E.J., Hay, W.W., and Thompson, S., 1989, The hydrologic cycle: A major variable during Earth history: Palaeogeography, Palaeoclimatology, Palaeoecology, v. 75, no. 3, p. 157–174, doi: 10.1016/0031-0182(89)90175-2.

Benammi, M., Alvarado-Ortega, J., and Urrutia-Fucugauchi, J., 2006, Magnetostratigraphy of the Lower Cretaceous strata in Tlayua Quarry, Tepexi de Rodríguez, state of Puebla, Mexico: Earth, Planets, and Space, v. 58, p. 1295–1302.

Brewer, R., 1964, Fabric and Mineral Analysis of Soils: New York, John Wiley and Sons, 470 p.

Chahine, M.T., 1992, The hydrologic cycle and its influence on climate: Nature, v. 359, p. 373–380, doi: 10.1038/359373a0.

Davis, J.M., Ludvigson, G.A., Ufnar, D.F., Atchley, S., Gonzalez, L.A., Brenner, R.L., and Witzke, B.J., 2004, Diagenetic analysis of a subaerial exposure surface from the Cretaceous (Albian) Walnut Formation, central Texas: Geological Society of America Abstracts with Programs, v. 36, p. 75.

Dunham, R.J., 1962, Classification of carbonate rocks according to their depositional texture, *in* Ham, W.E., ed., Classification of Carbonate Rocks—A Symposium: American Association of Petroleum Geologists Memoir 1, p. 108–121.

Espinosa-Arrubarrena, L., and Applegate, S.P., 1996, A paleoecological model of the vertebrate bearing beds in the Tlayua Quarries, near Tepexi de Rodríguez, Puebla, Mexico, *in* Arratia, G., and Viohl, G., eds., Mesozoic Fishes—Systematics and Paleoecology: Munich, Verlag, p. 539–550.

Folk, R.L., 1962, Spectral subdivision of limestone types, *in* Ham, W.E., ed., Classification of Carbonate Rocks—A Symposium: Tulsa, American Association of Petroleum Geologists Memoir 1, p. 62–84.

Friedman, I., and O'Neil, J.R., 1977, Compilation of stable isotope fractionation factors of geochemical interest: U.S. Geological Survey professional paper: Washington, DC, U.S. G.P.O., 440-KK, 12 p.

Gonfiantini, R., 1986, Environmental isotopes in lake studies, *in* Fritz, P.a.F., J.-Ch., ed., Handbook of Environmental Isotope Geochemistry: Volume 2. The Terrestrial Environment: Amsterdam, Elsevier, p. 113–168.

Graversen, R.G., Mauritsen, T., Tjernström, M., Källen, E., and Svensson, G., 2008, Vertical structure of recent arctic warming: Nature, v. 451, p. 53–57, doi: 10.1038/nature06502.

Hammer, Ø., Harper, D. A. T., and Ryan, P. D., 2008, PAST-Paleontological Statistics, version 1.79, Oslo, Norway, University of Oslo, 87 p.

Haywood, A.M., Valdes, P.J., and Markwick, P.J., 2004, Cretaceous (Wealden) climates: A modeling perspective: Cretaceous Research, v. 25, p. 303–311, doi: 10.1016/j.cretres.2004.01.005.

Heckel, P.H., 1972, Recognition of ancient shallow marine environments, *in* Rigby J.K., and Hamblin, W.K., eds., Recognition of Ancient Sedimentary Environments, A Symposium: Society of Economic Paleontologists and Mineralogists Special Publication 16, p. 226–286.

Kashiyama, Y., Fastovsky, D.E., Rutherford, S., King, J., and Montellano, M., 2004, Genesis of a locality of exceptional fossil preservation: Paleoenvironments of Tepexi de Rodríguez (mid-Cretaceous, Puebla, Mexico): Cretaceous Research, v. 25, p. 153–177, doi: 10.1016/j.cretres.2003.11.002.

Lohmann, K.C, 1988, Geochemical patterns of meteoric diagenetic systems and their application to studies of paleokarst, *in* James, N.P., and Choquette, P.W., eds., Paleokarst: New York, Springer, p. 58–80.

Ludvigson, G., González, L.A., Metzger, R.A., Witzke, B.J., Brenner, R.L., Murillo, A.P., and White, T.S., 1998, Meteoric sphaerosiderite lines and their use for paleohydrology and paleoclimatology: Geology, v. 26, no. 11, p. 1039–1042, doi: 10.1130/0091-7613(1998)026<1039:MSLATU>2.3.CO;2.

Ludvigson, G.A., Ufnar, D.F., González, L.A., Carpenter, S.J., Witzke, B.J., Brenner, R.L., and Davis, J., 2004, Terrestrial paleoclimatology of the Mid-Cretaceous greenhouse: I. Cross-calibration of pedogenic siderite & calcite $\delta^{18}O$ proxies at the Hadley cell boundary: Geological Society of America Abstracts with Programs, v. 36, no. 5, p. 305.

Malpica-Cruz, V.M., Pantoja-Alor, J., and Galguera-Rosas, G., 1989, Microfacies de la Cantera Tlayua, Puebla, Mexico: Primer Simposio sobre Geología Regional de México, v. 3, p. 53–56.

Martill, D., 1989, A new Solnhofen in Mexico: Geology Today, v. 5, p. 25–28, doi: 10.1111/j.1365-2451.1989.tb00607.x.

Meschede, M., and Frisch, W., 1998, A plate-tectonic model for the Mesozoic and early Cenozoic history of the Caribbean plate: Tectonophysics, v. 296, p. 269–291, doi: 10.1016/S0040-1951(98)00157-7.

Pantoja-Alor, J., 1992, Geología y paleoambientes de la Cantera Tlayua, Tepexi de Rodríguez, estado de Puebla: Instituto de Geología Revista, v. 9, p. 156–169.

Poulsen, C.J., Pollard, D., and White, T.S., 2007, General circulation model simulation of the $\delta^{18}O$ content of continental precipitation in the middle Cretaceous: A model-proxy comparison: Geology, v. 35, p. 199–202, doi: 10.1130/G23343A.1.

Retallack, G.J., 1997, A Colour Guide to Paleosols: New York, Wiley, 175 p.

Reynoso, V.H., 1997, A "beaded" sphenodontian (Diapsida: Lepidosauria) from the Early Cretaceous of central Mexico: Journal of Vertebrate Paleontology, v. 17, p. 52–59.

Reynoso, V.H., 2000, An unusual aquatic sphenodontian (Reptilia: Diapsida) from Tlayua Formation (Albian), central México: Journal of Paleontology, v. 74, p. 133–148, doi: 10.1666/0022-3360(2000)074<0133:AUASRD>2.0.CO;2.

Reynoso, V.H., 2006, Research on fossil amphibians and reptiles in Mexico from 1869 to early 2004 (including marine forms, but excluding pterosaurs, dinosaurs, and obviously birds), *in* Vega, F. J., Nyborg, T.G., Perrilliat, M.C., Montellano-Ballesteros, M., Cevallos-Ferriz, S.R.S., and Quiroz-Barroso, S.A., eds., Studies on Mexican Paleontology: Dordrecht, Springer, p. 209–226.

Shinn, E.A., 1983, Tidal flat environment, *in* Scholle, P.A., Bebout, D.G., and Moore, C.H., eds., Carbonate Depositional Environments: Tulsa, American Association of Petroleum Geologists, p. 171–210.

Sokal, R.R., and Rohlf, F.J., 1995, Biometry: The Principals and Practice of Statistics in Biological Research: New York, W.H. Freeman and Company, 887 p.

Sorensen, A. C., Ludvigson, G.A., González, L.A., Joeckel, R.M., and Kirkland, J.I., 2002, Petrography and diagenesis of palustrine carbonate beds in the Early Cretaceous Cedar Mountain Formation, eastern Utah: Geological Society of America Abstracts with Programs, v. 34, no. 6, p. 17–18.

Spicer, R.A., and Corfield, R.M., 1992, A review of terrestrial and marine climates in the Cretaceous with implications for modeling the "Greenhouse Earth": Geological Magazine, v. 2, p. 169–180.

Stoops, G., 2003, Guidelines for Analysis and Description of Soil and Regolith Thin Sections: Madison, Soil Science Society of America, 184 p.

Suarez, M., González, L.A., Ludvigson, G.A., and Davis, J., 2007, Pedogenic sphaerosiderites from the Caballos Formation (Aptian-Albian) of Colombia; a stable isotope proxy for Cretaceous paleoequatorial precipitation: Geological Society of America Abstracts with Programs, v. 39, no. 3, p. 75.

Ufnar, D.F., González, L.A., Ludvigson, G.A., Brenner, R.L., and Witzke, B.J., 2002, The mid-Cretaceous water bearer: Isotope mass balance quantification of the Albian hydrologic cycle: Palaeogeography, Palaeoclimatology, Palaeoecology, v. 188, p. 51–71, doi: 10.1016/S0031-0182(02)00530-8.

Ufnar, D.F., González, L.A., Ludvigson, G.A., Brenner, R.L., and Witzke, B.J., 2004, Evidence for increased latent heat transport during the Cretaceous (Albian) greenhouse warming: Geology, v. 32, no. 12, p. 1049–1052, doi: 10.1130/G20828.1.

Ufnar, D.F., Ludvigson, G.A., González, L.A., and Davis, J., 2005, Mid-Cretaceous evaporation rates estimated from pedogenic carbonate isotopic values in the Glen Rose Formation, Texas: Geological Society of America Abstracts with Programs, v. 37, no. 7, p. 357.

Ufnar, D.F., Gröcke, D.R., and Beddows, P.A., 2008, Assessing pedogenic calcite stable-isotope values: Can positive linear covariant trends be used to quantify palaeo-evaporation rates?: Chemical Geology, v. 256, p. 46–51, doi: 10.1016/j.chemgeo.2008.07.022.

White, T.S., González, L.A., Ludvigson Greg, A., and Poulsen, C.J., 2001, Middle Cretaceous greenhouse hydrologic cycle of North America: Geology, v. 29, p. 363–366, doi: 10.1130/0091-7613(2001)029<0363:MCGHCO>2.0.CO;2.

Wolfe, J.A., and Upchurch, G.J.R., 1987, North American nonmarine climates and vegetation during the Late Cretaceous: Palaeogeography, Palaeoclimatology, Palaeoecology, v. 61, p. 33–77, doi: 10.1016/0031-0182(87)90040-X.

Zhang, X., Zwiers, F.W., Hegerl, G.C., Lambert, F.H., Gillet, N.P., Soloman, S., Stott, P.A., and Nozawa, P., 2007, Detection of human influence on twentieth-century precipitation trends: Nature, v. 448, p. 461–466, doi: 10.1038/nature06025.

MANUSCRIPT RECEIVED 16 APRIL 2008
REVISED MANUSCRIPT RECEIVED 28 OCTOBER 2008
MANUSCRIPT ACCEPTED 6 NOVEMBER 2008

Printed in the USA